Research Article

Peng Zhang, Cong Wang, Fei Wang*, and Peng Yuan

Influence of sodium silicate to precursor ratio on mechanical properties and durability of the metakaolin/fly ash alkali-activated sustainable mortar using manufactured sand

https://doi.org/10.1515/rams-2022-0330 received February 28, 2023; accepted May 29, 2023

Abstract: In recent years, manufactured sand produced from crushed rock has been used as fine aggregate instead of natural sand in construction and industrial fields to minimize the impact of natural sand depletion in nature and society. In this research, the mechanical properties and durability of alkali-activated sustainable mortar using manufactured sand and different sodium silicate (solution) to precursor ratios (SSPR; 0.60, 0.65, 0.70, 0.75, and 0.80) by weight were investigated. Metakaolin and fly ash were used as precursor, sodium silicate (solution) and sodium hydroxide were used as alkali-activator, and manufactured sand made from broken limestone was used to completely replace river sand as fine aggregate to prepare metakaolin/fly ash (MK/FA) alkali-activated sustainable mortar to ensure sustainable development. The compressive, tensile, and flexural strengths, anti-permeability, and crack resistance of MK/FA alkali-activated sustainable mortar were tested. The impact of different SSPRs on the mechanical properties and durability of alkali-activated sustainable mortar was analyzed. Quadratic function fitting models of tensile strength to compressive strength and flexural strength to compressive strength were proposed. Furthermore, the statistical effects of each parameter were explored using analysis of variance and *F*-test of statistical analysis. The experimental results indicate that the SSPR has a remarkable effect on the mechanical properties and durability of MK/FA alkali-activated sustainable mortar. When the SSPR is in the range of 0.6-0.8, the compressive, tensile, and flexural strength of the alkali-activated sustainable mortar initially increased and then decreased;

however, there is an opposite trend in water penetration depth and crack index. MK/FA alkali-activated sustainable mortar exhibits best compressive strength, tensile strength, flexural strength, anti-permeability, and cracking resistance of 40.2 MPa, 3.38 MPa, 4.3 MPa, 41.3 mm, and 245 mm, respectively, at SSPR of 0.7. The experimental findings of this study can provide theoretical guidance for practical engineering of alkali-activated sustainable mortars using manufactured sand.

Keywords: alkali-activated sustainable mortar, sodium silicate to precursor ratio, manufactured sand, mechanical properties, durability

1 Introduction

In the last decades, the rapid acceleration of urbanization and industrialization has led to an increasing use of natural river sand and other construction materials for infrastructure construction [1]. According to statistics, about 5 billion tons of sand has been used annually for the preparation of concrete and mortar, and most of them are natural river sand, which has made natural river sand the most consumed natural resource on earth after fresh water and fossil fuels [2–5]. The uncontrolled mining of natural river sand has caused the exhaustion of river sand resources in many countries. And, the indiscriminate mining of river sand has resulted in irreversible impacts on the natural environment, ecosystem, and human society [6,7].

With the concept of sustainable development on the rise, using manufactured sand instead of natural sand in construction and industry has become a possibility to alleviate the depletion of river sand resources [8–10]. Manufactured sand is made from rock, gravel, and municipal construction waste through mechanical crushing. It is of interest to a wide range of construction industry practitioners because of its renewable nature, wide source, and

Peng Zhang, Cong Wang, Peng Yuan: Yellow River Laboratory, Zhengzhou University, Zhengzhou, 450001, China

^{*} Corresponding author: Fei Wang, Yellow River Laboratory, Zhengzhou University, Zhengzhou, 450001, China, e-mail: wangfei0826@163.com

2 — Peng Zhang et al. DE GRUYTER

low price. A lot of research results have shown that the use of manufactured sand to replace river sand as fine aggregate for preparing concrete or cement composites has yielded good results [10–13]. Shen et al. [2] presented a successful example of clean production of digital control manufactured sand for the Hechi-Baise Expressway. They found that the workability of the manufactured sand concrete was improved by an average of 16.19%, the strength was increased by an average of 7.1%, and it had excellent chloride ion penetration resistance. Khyaliya et al. [14] studied the impact of replacing river sand (0-100%) with marble waste as fine aggregate on mechanical and durability properties of mortar. Results revealed that the compressive strength improved from 2.84 to 7.04 MPa at 50% replacement. Furthermore, the appropriate amount of stone powder content in manufactured sand has a certain influence on the properties of concrete or mortar [9,10,15-19]. For example, Ji et al. [20] discovered that the compressive strength, tensile strength, and modulus of elasticity of manufactured sand concrete gradually increased with the increase in the content of fine stone powder. Hence, it is feasible to use manufactured sand instead of natural sand in the construction industry.

As a new, eco-friendly, and sustainable alternative to ordinary cement construction material, geopolymer is receiving increasing attention in the construction industry due to its wide range of sources, good mechanical properties, and excellent durability [21–35]. Geopolymer is usually produced by polymerizing industrial by-products rich in silica and alumina as precursor (i.e., metakaolin [MK], bottom ash, fly ash [FA], blast furnace slag, etc.) with alkali-activator solution. Studies have demonstrated that the use of geopolymer as new building materials can significantly reduce greenhouse gas emissions and energy consumption [36-41]. Moreover, it has been shown that geopolymer using two or more raw materials has higher performance than that using only one raw material [42–45]. Generally, alkali-activator solution is prepared using sodium silicate and sodium hydroxide. Soluble alkali-activator solution can enhance the hydration reaction during polymerization and promote the formation of the new hydrated phase [46]. In the preparation of geopolymer, activator to precursor ratio is an extremely critical factor for the formation of stable geopolymer, which determines the workability, fresh properties, mechanical properties, and durability of the mixtures [46,47]. Kanagaraj et al. [47] revealed that the ratio of alkali-activator to binder significantly affected the properties of geopolymer. When the alkali-activator to binder ratio was 0.36-0.74, the density, slump, and compressive strength all increased and the water absorption reduced. Although many researchers have analyzed the impact of activator to binder ratio on the reaction mechanism, mechanical properties, and durability of geopolymer mortar, there are still insufficient research works on the influence of sodium silicate to precursor ratio (SSPR) on the properties of MK/FA alkali-activated sustainable mortar using manufactured sand.

In order to achieve sustainable development in the construction industry, this study used manufactured sand to completely replace natural sand in preparing MK/FA alkali-activated sustainable mortar. The effect of SSPR on the performance of alkali-activated sustainable mortar was investigated. The compressive, tensile, and flexural strength, anti-permeability, and crack resistance of alkaliactivated sustainable mortar were investigated by various tests. In addition, the relation of tensile strength to compressive strength and flexural strength to compressive strength of alkali-activated sustainable mortar was proposed. Finally, statistical analysis (analysis of variance and F-test) was used to determine the influence of SSPR on the performance of alkali-activated sustainable mortar based on the test data of this study. The results of this study can provide a reference for the engineering application of alkali-activated sustainable mortars with manufactured sand.

2 Materials and methodology

2.1 Materials

In this study, MK/FA alkali-activated sustainable mortar was prepared using MK, FA, sodium silicate, sodium hydroxide, manufactured sand, and water. MK and FA were used as precursor for the preparation of MK/FA alkali-activated sustainable mortars. MK with an average particle size of approximately 1.2 mm was sourced from Chenxing Industrial Co. Ltd, Shijiazhuang City, China. Class I FA was supplied by the power plant in Luoyang City, China. The main chemical compositions of the two raw materials are presented in Table 1. The alkali-activator was composed of sodium silicate (Longxiang Ceramics Co. Ltd, Zhengzhou City, Henan Province, $SiO_2/Na_2O = 3.2$, specific gravity of 1.38 g·cm⁻³, 34.3% solid content) and sodium hydroxide (Jinhai Xinwu Fine Chemical Co. Ltd, Ningxia, China, 99% purity). Manufactured sand was sourced from broken limestone which is manufactured by Changshen Manufactured Sand Co. Ltd, Xinxiang City, China. And a certain amount of stone powder was produced in the production process of manufactured sand. The moderate dosage of stone powder not only improves the workability of the mix, but also improves the compressive

Table 1: Chemical compositions of MK and FA (wt%)

Chemical composition	SiO ₂	Fe ₂ O ₃	Al ₂ O ₃	SO₃	CaO and MgO	Na ₂ O and K ₂ O	Other
MK	53.0	1.3	43.0	_	≤0.8	≤0.7	≥1.2
FA	51.5	6.7	18.5	0.21	12.5	4.4	6.19

strength of the geopolymer [18,19]. In this study, the content of stone powder (by mass) is 6%. Table 2 demonstrates the physical performance of the manufactured sand blended with stone powder.

2.2 Mixing proportions and specimen preparation

MK and FA were at first dried in a drying oven for 24 h to clean the water from the surface. Then, the raw materials were mixed in a certain ratio to prepare the cementitious material. The MK/FA ratio has a remarkable impact on the mechanical performance of geopolymer mortar [26,44,48,49]. In the previous study, the best mechanical properties of the geopolymer mortar were obtained at a MK/FA ratio of 7:3 [3,21]. In this study, the precursor consisted of 70% MK and 30% FA (by weight). Manufactured sand was dried in the natural state to remove the free water adhering to the surface. The weight ratio of precursor to manufactured sand was consistently 1. Flaky sodium hydroxide was added to the sodium silicate solution having a molar ratio of 3.2 and both were mixed thoroughly under the assistance of a mechanical stirrer. The ratios of sodium silicate to precursor (by weight) were 0.60, 0.65, 0.70, 0.75, and 0.80. More details about the mixing proportions of the MK/FA alkali-activated sustainable mortar are provided in Table 3.

Initially, the alkali-activated solution was prepared 24 h before casting and the prepared alkali-activated solution was stored at the room temperature. The dried compound mixture was first mixed with manufactured sand and stirred for 3 min. Then, the prepared alkali-activator was added to the mixture and stirred for 2-3 min until proper fluidity was obtained. After testing the workability of the mixture, the mixture was immediately moved to molds of different sizes, vibrated, and left at room temperature for 1 day. Eventually, the demolded specimens were cured in a standard maintenance box at 20 ± 2°C for 28 days. MK/FA alkali-activated sustainable mortar fabrication is illustrated in Figure 1.

2.3 Experimental methods

2.3.1 Mechanical properties

The cubic compressive strength test (cube specimen: $70.7 \times$ 70.7×70.7 mm), splitting tensile strength test (cube specimen: $70.7 \times 70.7 \times 70.7$ mm), and flexural strength test (prism specimen: $40 \times 40 \times 160$ mm) were performed on

Table 2: Physical performance of manufactured sand blended with stone powder

Properties Fineness modulus		Stone powder (%)	Apparent density (kg·m ^{−3})	Water absorption (%)	
Values	2.8	6	1,820	4.5	

Table 3: Mix proportions of alkali-activated sustainable mortar

Mix ID	Precursor (kg·m ^{−3})		Water (kg·m ^{−3})	Alkali-acti	vator (kg·m ^{−3})	Manufactured sand (kg·m ⁻		
	MK	FA		Na ₂ SiO ₃	NaOH			
N-0.60	429	184	189	368	56.9	613		
N-0.65	429	184	145	399	64	613		
N-0.70	429	184	100	430	71.2	613		
N-0.75	429	184	70	460	78.2	613		
N-0.80	429	184	50	491	85.4	613		

4 — Peng Zhang et al. DE GRUYTER

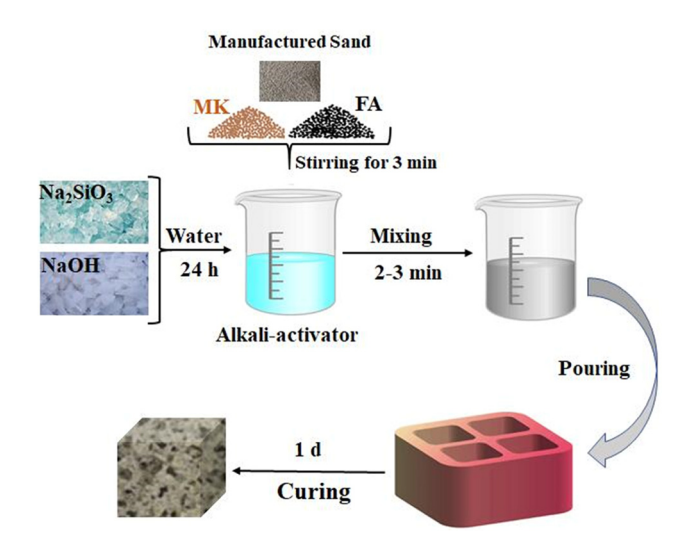


Figure 1: Process flow diagram of alkali-activated sustainable mortar.

28th day following the Chinese standard JGJ/T 70-2009 [50], GB/T 7897-2008 [51], and GB/T 7897-2008, respectively. A pressure testing machine with a range of 2,000 kN controlled by a microcomputer (Hualong Testing Instruments Co., Ltd, Shanghai City, China) was used to test the different sizes of specimens. The loading rate was $1\,\mathrm{kN}\cdot\mathrm{s}^{-1}$ for the cubic compressive strength test and splitting tensile strength test and 50 N·s⁻¹ for the flexural strength test. Mechanical strength test was completed until damage occurred to the specimen. Three samples were prepared for each mixing proportion and the average of the three specimen strengths was used as the final strength for each test.

2.3.2 Anti-permeability

The water penetration resistance test using Chinese standard GB/T 50082-2009 [52] was performed using a circular table body mold with an internal diameter of 175 mm at the top, 185 mm at the bottom, and a height of 150 mm. The impermeability tester is presented in Figure 2. Six specimens were cast for each set of ratios. The day before the test started, the samples were taken out from the maintenance room, and the water and dirt on the surface of the specimens were cleaned. The specimens were sealed with cement and butter in a mass ratio of 2.5:1. The sealed specimens were installed on the anti-permeability instrument, and the valve was opened to make the water pressure stable at 1.2 MPa within 24 h. Finally, the specimens taken out from the anti-permeability instrument were put on the machine for the splitting test, and the water penetration height values on the splitting surface of the specimen were recorded.



Figure 2: Appearance of impermeability tester.

The average depth of water permeability for each mixing proportion after 28 days of curing in this study was calculated by Eqs (1) and (2):

$$\bar{h}_i = \frac{1}{10} \sum_{j=1}^{10} h_j,\tag{1}$$

$$\bar{h} = \frac{1}{6} \sum_{i=1}^{6} \bar{h}_i,\tag{2}$$

where, h_j is the j-th testing spot of i-th sample water penetration height (mm); \bar{h}_i is the average water penetration height of the i-th sample (mm); \bar{h} is each set of 6 samples of average water penetration height (mm).

2.3.3 Crack resistance

A standard mold of 910 mm in length, 600 mm in width, and 20 mm in height was used for the crack resistance test referring to Chinese standard JC/T 951-2005 [53]. A twolayer PVA film was placed at the bottom of the mold to reduce the influence of the bottom of the mold on the shrinkage and deformation of the specimen. A light round steel frame with a diameter of 8 mm is placed inside the mold. The test room conditions should be controlled at the temperature of 20 \pm 3°C and relative humidity of 60 \pm 5%. A rag was used to clean the surface of the mold before casting the specimens. The mixture was cast homogeneously along the edge of the mold toward the center. After casting, the fan was switched on at once to cool the specimens. The wind speed of the fan should be controlled at $4.5 \pm 0.5 \,\mathrm{m\cdot s^{-1}}$. Meanwhile, iodine tungsten lamps with a power of 1,000 W were switched on to illuminate the

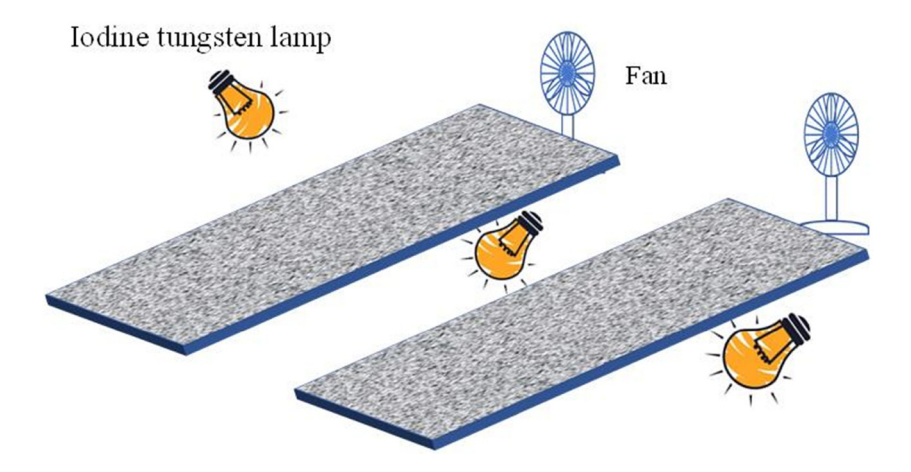


Figure 3: Schematic diagram of the test arrangement.

specimen for 4 h. Figure 3 illustrates the diagram of the test arrangement.

The number, length, and width of cracks on the surface of the specimens after 24 h were measured and recorded. The average cracking index of the two specimens was used as the cracking index (*W*) for each group of specimens in this study. *W* can be described as Eq. (3).

$$W = \sum (A_i \cdot l_i), \tag{3}$$

where W is the specimen cracking index; A_i is the weight value corresponding to each crack, and more details are listed in Table 4; l_i is the length of each crack on the surface of the specimen.

3 Experimental results and discussion

3.1 Mechanical properties of alkali-activated sustainable mortar

3.1.1 Cube compressive strength

The impact of SSPR on the compressive strength of alkaliactivated sustainable mortar is presented in Figure 4. It can be found that the compressive strength of the alkali-activated

Table 4: Weight (A) corresponding to the crack width (d)

d (mm)	<i>d</i> < 0.5	0.5 ≤ <i>d</i> < 1	1 ≤ <i>d</i> < 2	2 ≤ <i>d</i> < 3	3 ≤ <i>d</i>
A	0.25	0.5	1	2	3

sustainable mortar depends on the SSPR to some extent. The compressive strength of alkali-activated sustainable mortar showed a trend of increasing first and then decreasing as the SSPR increased from 0.6 to 0.8. When the SSPR was 0.7, the maximum compressive strength of alkali-activated sustainable mortar was 40.2 MPa. However, when the SSPR was 0.6, 0.65, 0.75, and 0.8, the compressive strength of alkali-activated sustainable mortar decreased by 33.3, 19.4, 8.5, and 17.7%, respectively, compared with the maximum value.

A similar finding was gained by Ishwarya *et al.*, who revealed that the compressive strength of FA/slag geopolymer pastes at 28 days first increased and then gradually decreased as the amount of activator increased [37]. Moreover, Kanagaraj *et al.* [47] investigated the effect of alkaliactivator to binder ratios on the properties of geopolymer

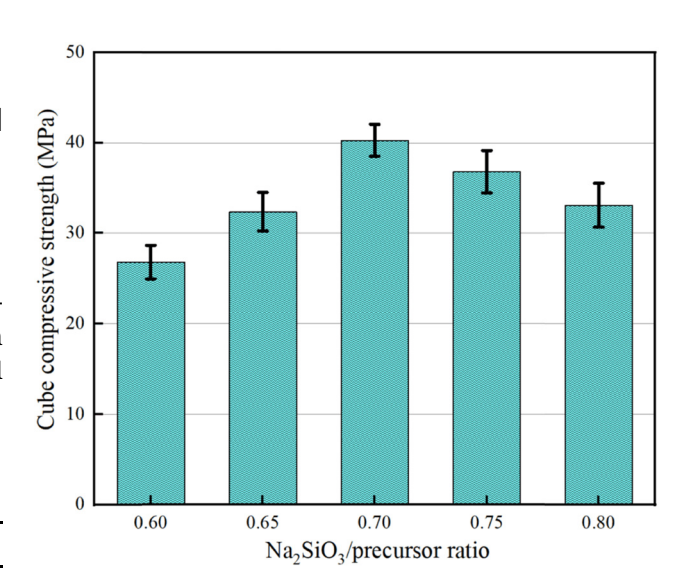


Figure 4: Effect of SSPR on compressive strength.

with conventional sand, and they discovered that the compressive strength of geopolymers improved from 37.3 to 44.4 MPa as the alkali-activator to binder ratio increased from 0.36 to 0.74. The maximum compressive strength of the geopolymer using conventional sand is slightly higher than that of the geopolymer mortar using manufactured sand, which may be due to the irregular shape of the manufactured sand and the fact that the surface contains many open pores [54].

Figure 5 exhibits the damage patterns of the alkaliactivated sustainable mortar at SSPR of 0.6, 0.7, and 0.8, respectively. It can be clearly seen that the damage of the specimens with a high SSPR is more severe than that of the specimens with a low SSPR. The mechanism of the influence of SSPR on the compressive strength of alkali-activated sustainable mortar is discussed below.

The reaction of MK/FA geopolymer mortar is a polymerization reaction with multiple depolymerization and condensation, where the alkali-activator provides the necessary alkaline environment [46,55]. Meanwhile, the alkali-activator also plays an important role in regulating the flow of the mixture. The low ratio is accompanied by a low Si-Al molar ratio, which means that the Si content in the alkaliactivator is insufficient, resulting in the polymerization reaction of the MK/FA geopolymer mortar becoming incomplete. Moreover, the low compressive strength of alkali-activated sustainable mortars may also be due to the low content of alkali in the alkali-activator [54,56,57]. The insufficient alkali dosage in the alkali-activator does not provide an optimal alkali environment for the geopolymer reaction, resulting in the inability to generate a sufficient amount of N-A-S-H gels in the geopolymer reaction. The appropriate amount of sodium silicate solution can dissolve, depolymerize, and polycondense the silicate and aluminate oligomers sufficiently to produce -Si-O-Al-O-Si- and -Si-O-Al-O-Si-O-Si- in the matrix. These reticular structures are cross-linked to

each other, making the internal structure of MK/FA alkali-activated sustainable mortar much denser, thus improving the compressive strength of alkali-activated sustainable mortar [58]. With the increase in the SSPR, the excess Na_2SiO_3 in the alkali-activator cannot react with the free SiO_2 in the paste, resulting in the formation of hardened crystals in the geopolymer mortar. Simultaneously, the excess alkali in the alkali-activator may also interact with CO_2 and H_2O in the air to generate sodium carbonate crystals precipitated on the surface of the silica-aluminate, thus affecting the denseness of the alkali-activated sustainable mortar.

3.1.2 Splitting tensile strength and flexural strength

The effect of SSPR on the tensile strength and flexural strength of alkali-activated sustainable mortar is depicted in Figures 6 and 7, respectively. It can be clearly found that the tendency of tensile strength and flexural strength of alkali-activated sustainable mortar is consistent with that of compressive strength. When the SSPR increased from 0.6 to 0.7, the tensile and flexural strength of MK/FA alkali-activated sustainable mortar both increased, and the strength gradually decreased as the ratio continued to increase. When the SSPR was 0.7, the tensile and flexural strength of MK/FA alkali-activated sustainable mortar reached the maximum values of 3.38 and 4.3 MPa, respectively. Nevertheless, when the ratio was 0.6, 0.65, 0.75, and 0.8, the tensile strength decreased by 39.5, 27.9, 14, and 23.3%, respectively, compared with the maximum values, and the flexural strength decreased by 42, 25.1, 4.1, and 17.8%, respectively, compared with the maximum values.

The mechanism of the influence of the SSPR on the tensile and flexural strengths of alkali-activated sustainable mortar is similar. Specifically, when the ratio is below 0.7, the low strength of alkali-activated sustainable mortar can

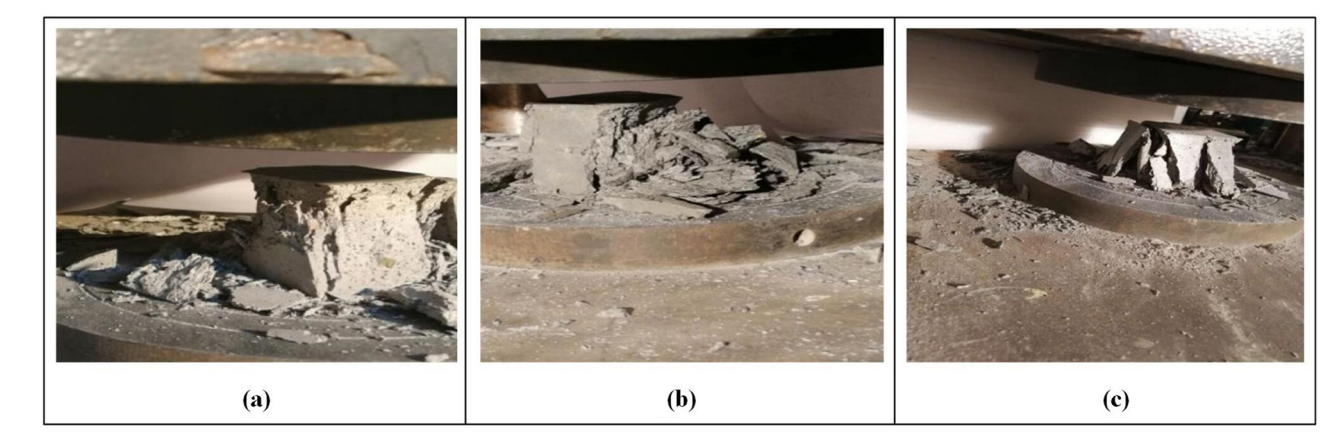


Figure 5: Damage state of specimens when SSPRs are (a) 0.6, (b) 0.7, and (c) 0.8, respectively.

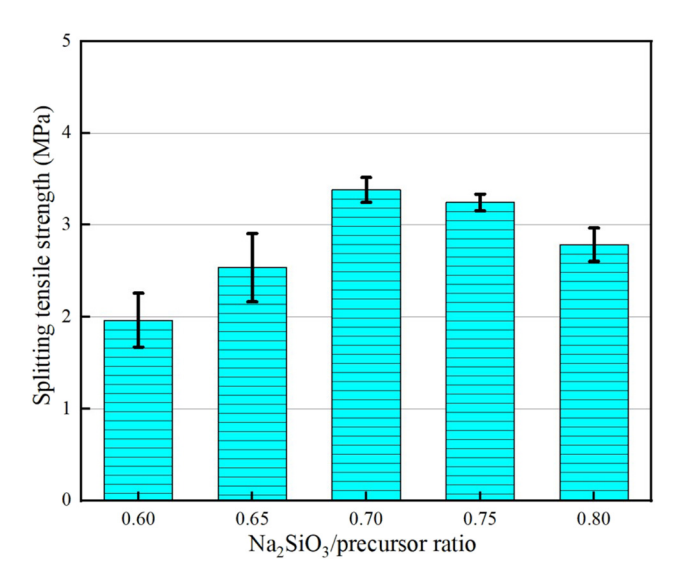


Figure 6: Effect of SSPR on splitting tensile strength.

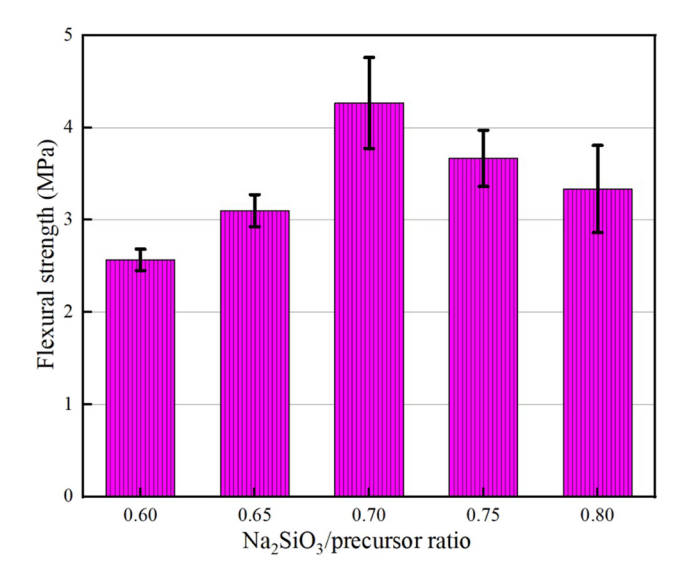


Figure 7: Effect of SSPR on flexural strength.

be attributed to the insufficient amount of alkali-activator, which leads to the inability to generate an amount of gels in the geopolymer mortar. When the ratio exceeds 0.7, the excess Na₂SiO₃ in the geopolymer mortar prevents the binder from fully polymerizing, which causes a reduction in the strength of the alkali-activated sustainable mortar.

3.1.3 Relationship of splitting tensile, flexural, and compressive strengths

In previous studies, many researchers have concluded that there is a relation between compressive strength and tensile strength, and compressive strength and flexural strength of geopolymer mortar [57,59–62]. Currently, there are various fitting models that have been used by researchers to model the relationship of compressive, tensile, and flexural strengths of geopolymer mortar or concrete based on experimental data, *i.e.*, quadratic function fitting model, power function fitting model, and exponential function fitting model, and so on. In this study, the quadratic function fitting model was used for alkali-activated sustainable mortar. According to the experimental results, the functional expressions of tensile, flexural, and compressive strength of MK/FA alkali-activated sustainable mortar are illustrated in Eqs (4) and (5).

$$f_{\rm t} = -0.0034 f_{\rm c}^2 + 0.334 f_{\rm c} - 4.59,$$
 (4)

$$f_{\rm f} = 0.0035 f_{\rm c}^2 - 0.108 f_{\rm c} + 2.97,$$
 (5)

where, f_t represents the splitting tensile strength; f_f represents the flexural strength; and f_c represents the compressive strength.

Figure 8a and b demonstrates the relation of tensile strength to compressive strength and flexural strength to compressive strength of alkali-activated sustainable mortar, respectively. It can be clearly found that there is an excellent connection between tensile strength, flexural strength, and compressive strength of MK/FA alkali-activated sustainable mortar. In addition, it is also found that the tensile strength of MK/FA alkali-activated sustainable mortar increases slowly with the increase in the compressive strength, while the flexural strength increases sharply with the increase in the compressive strength. The equation's correlation coefficient (R^2) indicates the total degree of variation of the dependent variable of the regression equation, which better explains the correlation of the fitted equation. Generally, the correlation of the regression equation is considered to be better when R^2 is closer to 1. In this study, the R^2 of tensile strength vs compressive strength of alkali-activated sustainable mortar is 0.945, and the R^2 of flexural strength vs compressive strength is 0.944. Hence, the quadratic function fitting equation derived from the experimental data can better reflect the relation of tensile strength to compressive strength and flexural strength to compressive strength of alkali-activated sustainable mortar.

3.2 Durability of alkali-activated sustainable mortar

3.2.1 Anti-permeability

Figure 9 demonstrates the influence of SSPR on the antipermeability of MK/FA alkali-activated sustainable mortar. It can be obviously found that the SSPR has a remarkable 8 — Peng Zhang et al. DE GRUYTER

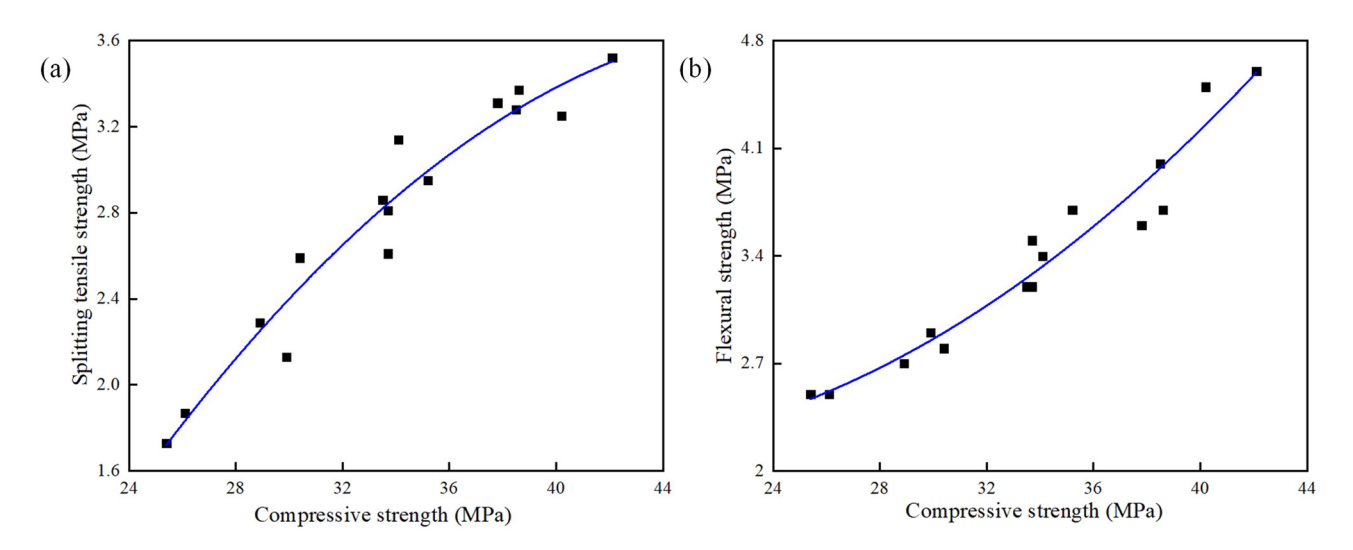


Figure 8: Relationship of tensile, flexural, and compressive strength: (a) relation between tensile and compressive strength; (b) relation between flexural and compressive strength.

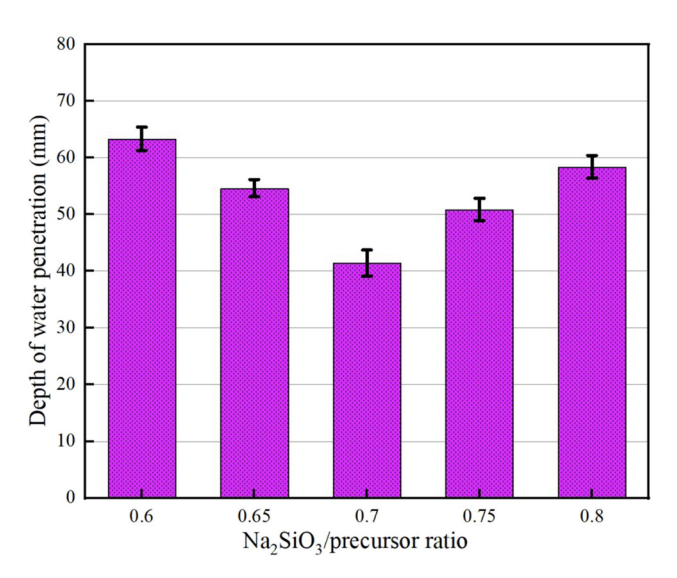


Figure 9: Effect of SSPR on the impermeability.

effect on the anti-permeability of the alkali-activated sustainable mortar. Specifically, the water penetration depth of alkali-activated sustainable mortar decreased as the SSPR increased from 0.6 to 0.7, and then gradually increased when the SSPR exceeded 0.7. The anti-permeability of the alkali-activated sustainable mortar was lowest with a mean water permeability depth of 41.3 mm at a SSPR of 0.7. However, at SSPR of 0.6, 0.65, 0.75, and 0.8, the mean permeability depth increased by 53.3, 32.2, 23, and 42.1%, respectively, compared to the minimum value. Similarly, Atabey *et al.* [63] discovered that the permeability depth of the specimens decreased with the increase in the sodium

ratio in the alkali-activated solution, especially the specimens with a higher depth of permeability at a Na ratio of 6%. Hedegaard and Hansen [64] proposed that the material can be considered impermeable with the maximum permeability depth below 50 mm. In this work, the average permeability depth and a maximum permeability depth of the specimens with a SSPR of 0.7 meet the above results. The reason for the low permeability depth can be attributed to the volcanic ash effect of fly ash and the dense effect of MgO [65–68]. Hence, the MK/FA alkali-activated sustainable mortar with a SSPR of 0.7 can be considered as a waterproofing material in practical construction projects.

3.2.2 Crack resistance

The effect of the SSPR on the crack resistance of alkaliactivated sustainable mortar is depicted in Figure 10. It can be found that the effect of the SSPR on the crack resistance of alkaliactivated sustainable mortar is consistent with the impermeability of alkaliactivated sustainable mortar. When the ratio increased from 0.6 to 0.8, the cracking index of alkaliactivated sustainable mortar initially decreased and then increased. When the SSPR was 0.7, the cracking index of alkaliactivated sustainable mortar was the smallest at 245 mm, and the specimen had the strongest crack resistance. When the ratio of sodium silicate to precursor was 0.6, 0.65, 0.75, and 0.8, the cracking index of the specimens increased by 55.9, 32.2, 45.3, and 82.4%, respectively, compared with the minimum value.

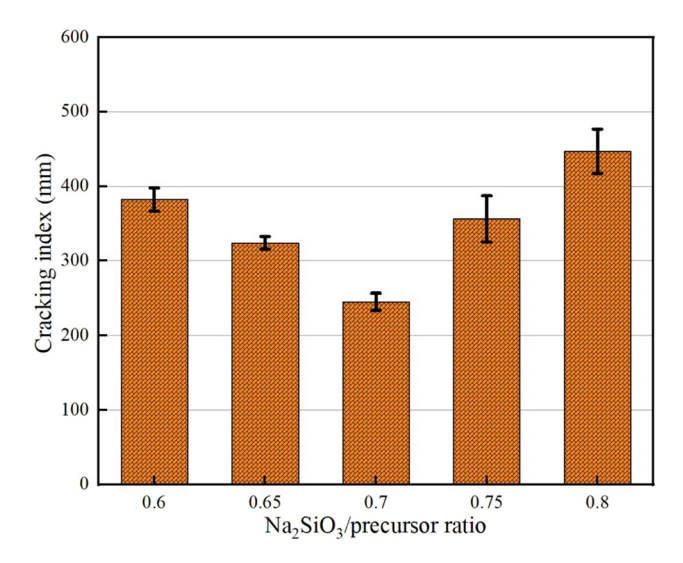


Figure 10: Effect of SSPR on the crack resistance.

3.2.3 Mechanism for durability of alkali-activated sustainable mortar

Anti-permeability and crack resistance are important indicators to evaluate the durability of geopolymers or concrete. In this study, the anti-permeability and crack resistance of MK/FA alkali-activated sustainable mortar are principally correlated with the matrix structure and internal pore structure of the mixes [66,69–73].

In MK/FA alkali-activated sustainable mortar, the refinement of the slurry's pore structure is mainly through the volcanic ash reaction of fly ash and gelation produced during

the polymerization reaction [66,74]. When the SSPR is at a low level (below 0.7), there is an insufficient amount of alkaliactivator in the matrix, especially the dosage of alkali, resulting in lower solubility of fly ash particles [75]. Meanwhile, the lower dose of alkali is not able to provide an optimal environment for the polymerization reaction, which results in an incomplete geopolymer reaction. When the SSPR is 0.7, the proper amount of alkali promotes the depolymerization and condensation reaction of the geopolymer and accelerates the generation of gels. In addition, it promotes the volcanic ash reaction of fly ash, which makes the microstructure of the paste much denser and more robust. When a higher SSPR is used, the dissolution rate of the raw material can be accelerated and the depolymerization and condensation reactions can be accelerated in a higher amount of alkali environment, but it also leads to the creation of zeolite-like structures [76]. Simultaneously, the excess OH ions in the MK/FA alkali-activated sustainable mortar paste negatively affect the activation process during the geopolymer reaction, resulting in a weak internal structure of the geopolymer paste [62].

4 Statistical analysis

Analysis of variance in statistical analysis was used to statistically process the experimental data in this study to evaluate more graphically and clearly the influence of SSPR on the mechanical and durability properties of

Table 5: Analysis of variance for different parameters

Parameters	N _{sample}	N _{Level}	Control factors	Sum of square (SS _{Level} / SS _{error})	Degrees of freedom	Mean square (MS _{Level} / MS _{error})	Calculated <i>F</i> -ratio	Critical <i>F</i> -ratio (α = 0.05)	Significance level	Critical <i>F</i> -ratio (α = 0.025)	Significance level
Compressive	15	5	SSPR	279.47	4	69.87	9.42	3.48	Significance	4.47	Significance
strength			Error	74.22	10	7.42	_	_		_	
			Total	353.69	14	_	_	_		_	
Tensile	15	5	SSPR	3.64	4	0.91	10.96	3.48	Significance	4.47	Significance
strength			Error	0.83	10	0.083	_	_		_	
			Total	4.47	14	_	_	_		_	
Flexural	15	5	SSPR	3.95	4	0.99	4.78	3.48	Significance	4.47	Significance
strength			Error	2.07	10	0.207	_	_		_	
			Total	6.02	14	_	_	_		_	
Depth of	30	5	SSPR	1414.76	4	353.69	26.47	2.76	Significance	3.35	Significance
water			Error	333.96	25	13.36	_	_		_	
penetration			Total	1748.72	29	_	_	_		_	
Cracking	10	5	SSPR	39269.37	4	9817.34	6.67	5.19	Significance	7.39	Insignificance
index			Error	7356.23	5	1471.25	_	_		_	
			Total	46625.6	9	_	_	_		_	

MK/FA alkali-activated sustainable mortar. Analysis of variance adopts the form of the sum of squares to determine the effect of test factors on test indicators, and it is widely used in a variety of fields [3,77–79]. The F-test in the hypothesis test was also used to test the significance level of SSPR on various properties of alkali-activated sustainable mortar. In the F-test, SS_{Level} represents the difference between the sample mean and the total mean of the data; MS_{Level} represents the number of factors; SS_{error} represents the difference between the sample value and the sample mean; MS_{error} represents the mean square of SS_{error} ; N_{sample} represents the all specimen counts.

The analysis of variance results for different SSPRs on the compressive strength, tensile strength, flexural strength, anti-permeability, and crack resistance of alkali-activated sustainable mortar are listed in Table 5. In this study, F-tests were conducted for the test parameters using significance levels $\alpha = 0.05$ and $\alpha = 0.025$, respectively. A higher level of significance represents a higher probability of the overall parameter falling in that interval to make an error. The calculated F-ratio is greater than the critical F-ratio at a significance level of 0.05, which implies that the SSPR has a remarkable effect on the mechanical and durability properties of alkali-activated sustainable mortar in the range of 0.6-0.8. At a significance level of 0.025, the calculated Fratios for compressive, tensile, flexural strength, and antipermeability of the alkali-activated sustainable mortar are all greater than the critical F-ratios, except for the calculated F-ratio for crack resistance. This indicates that the influence of the SSPR on the crack resistance of MK/FA alkali-activated sustainable mortar may become significant when the SSPR is beyond the test range at a significance level of 0.025. Hence, further experimental and theoretical studies are needed for related issues in future work.

5 Conclusion and potential work

In this study, the effect of SSPR on the mechanical properties and durability of the MK/FA alkali-activated sustainable mortar was investigated. In addition, statistical analysis was used in this study to evaluate the significant level of SSPRs on the mechanical and durability properties of MK/FA alkali-activated sustainable mortar. The conclusions obtained are as follows:

 The strengths of MK/FA alkali-activated sustainable mortar initially increased and then decreased as the SSPR varied from 0.6 to 0.8. The highest compressive, tensile, and flexural strength of 40.2, 3.38, and 4.3 MPa, respectively, were

- obtained at a ratio of 0.7 of sodium silicate to precursor. Moreover, the relation of tensile strength to compressive strength and flexural strength to compressive strength of MK/FA alkali-activated sustainable mortar can be better characterized by the quadratic function fitting models.
- 2) The results demonstrated that the water penetration depth and cracking index of MK/FA alkali-activated sustainable mortar first decreased and then increased when the SSPR was in the range of 0.6–0.8. In addition, MK/FA alkali-activated sustainable mortar exhibited the best anti-permeability and crack resistance at a ratio of 0.7 of sodium silicate to precursor, and the permeability depth and crack index of alkali-activated sustainable mortar were 41.3 and 245 mm, respectively.
- 3) The analysis of variance and F-test results revealed that the SSPR had a significant effect on the compressive strength, tensile strength, flexural strength, anti-permeability, and crack resistance of MK/FA alkali-activated sustainable mortar at the significance level $\alpha = 0.05$.

Based on the research of this work, considering the influence of the external environment on the structure, possible future work is as follows. The effect of SSPR on the mechanical properties and durability of the specimens in terms of compressive, tensile, erosion, penetration, high temperature, and impact resistance at the microscopic level is recommended for further study and analysis in future work.

Acknowledgments: The authors would like to thank all the editors and the anonymous referees for their constructive comments and suggestions.

Funding information: The authors would like to acknowledge the financial support received from National Natural Science Foundation of China (Grant Nos. 52278283 and U2040224), Natural Science Foundation of Henan Province of China (Grant No. 212300410018), and Project Special Funding of Yellow River Laboratory (Grant No. YRL22LT02).

Author contributions: All authors have accepted responsibility for the entire content of this manuscript and approved its submission.

Conflict of interest: The authors state no conflict of interest.

References

 Srivastava, A. and S. K. Singh. Utilization of alternative sand for preparation of sustainable mortar: a review. *Journal of Cleaner Production*, Vol. 253, 2020, id. 119706.

- [2] Shen, W., J. Wu, X. Du, Z. Li, D. Wu, J. Sun, et al. Cleaner production of high-quality manufactured sand and ecological utilization of recycled stone powder in concrete. Journal of Cleaner Production, Vol. 375, 2022, id. 134146.
- Zhang, P., L. Y. Kang, Y. X. Zheng, T. H. Zhang, and B. Zhang. Influence of SiO₂/Na₂O molar ratio on mechanical properties and durability of metakaolin-fly ash blend alkali-activated sustainable mortar incorporating manufactured sand, *Journal of Materials* Research and Technology, Vol. 18, 2022, pp. 3553-3563.
- Koehnken, L., M. S. Rintoul, M. Goichot, D. Tickner, A. C. Loftus, and M. C. Acreman. Impacts of riverine sand mining on freshwater ecosystems: a review of the scientific evidence and guidance for future research. River Research and Applications, Vol. 36, 2020, pp. 362-370.
- [5] Zhang, P., M. H. Wang, X. Han, and Y. X. Zheng. A review on properties of cement-based composites doped with graphene. Journal of Building Engineering, Vol. 70, 2023, id. 106367.
- Zheng, Y. X., J. B. Zhuo, P. Zhang, and M. Ma. Mechanical properties and meso-microscopic mechanism of basalt fiber-reinforced recycled aggregate concrete. Journal of Cleaner Production, Vol. 370, 2022, id. 133555.
- Abdalla, A. and A. Salih. Implementation of multi-expression programming (MEP), artificial neural network (ANN), and M5P-tree to forecast the compression strength cement-based mortar modified by calcium hydroxide at different mix proportions and curing ages. Innovative Infrastructure Solutions, Vol. 7, 2022, id. 153.
- Cepuritis, R., B. J. Wigum, E. J. Garboczi, E. Mortsell, and S. Jacobsen. [8] Filler from crushed aggregate for concrete: Pore structure, specific surface, particle shape and size distribution. Cement & Concrete Composites, Vol. 54, 2014, pp. 2-16.
- Shen, W. G., Y. Liu, Z. W. Wang, L. H. Cao, D. L. Wu, Y. J. Wang, et al. Influence of manufactured sand's characteristics on its concrete performance. Construction and Building Materials, Vol. 172, 2018, pp. 574-583.
- [10] Nanthagopalan, P. and M. Santhanam. Fresh and hardened properties of self-compacting concrete produced with manufactured sand. Cement & Concrete Composites, Vol. 33, 2011,
- [11] Arulmoly, B., C. Konthesingha, and A. Nanayakkara. Performance evaluation of cement mortar produced with manufactured sand and offshore sand as alternatives for river sand. Construction and Building Materials, Vol. 297, 2021, id. 123784.
- [12] Donza, H., O. Cabrera, and E. F. Irassar. High-strength concrete with different fine aggregate. Cement and Concrete Research, Vol. 32, 2002, pp. 1755-1761.
- [13] Li, B. X., G. J. Ke, and M. K. Zhou. Influence of manufactured sand characteristics on strength and abrasion resistance of pavement cement concrete. Construction and Building Materials, Vol. 25, 2011, pp. 3849-3853.
- [14] Khyaliya, R. K., K. Kabeer, and A. K. Vyas. Evaluation of strength and durability of lean mortar mixes containing marble waste. Construction and Building Materials, Vol. 147, 2017, pp. 598-607.
- [15] Zhang, Y. Z., L. Y. Gu, and Q. L. Zhang. Durability of manufactured sand concrete in atmospheric acidification environment. Case Studies in Construction Materials, Vol. 17, 2022, id. e01613.
- [16] Zhao, S. B., X. X. Ding, M. S. Zhao, C. Y. Li, and S. W. Pei. Experimental study on tensile strength development of concrete with manufactured sand. Construction and Building Materials, Vol. 138, 2017, pp. 247-253.

- [17] Bonavetti, V., H. Donza, G. Menendez, O. Cabrera, and E. F. Irassar. Limestone filler cement in low W/C concrete: A rational use of energy. Cement and Concrete Research, Vol. 33, 2003, pp. 865-871.
- [18] Li, B. X., J. L. Wang, and M. K. Zhou. Effect of limestone fines content in manufactured sand on durability of low- and high-strength concretes. Construction and Building Materials, Vol. 23, 2009, pp. 2846-2850.
- [19] Ding, X. X., C. Y. Li, Y. Y. Xu, F. L. Li, and S. B. Zhao. Experimental study on long-term compressive strength of concrete with manufactured sand. Construction and Building Materials, Vol. 108, 2016,
- [20] Ji, T., C. Y. Chen, Y. Z. Zhuang, and J. F. Chen. A mix proportion design method of manufactured sand concrete based on minimum paste theory. Construction and Building Materials, Vol. 44, 2013,
- [21] Zhang, P., X. Han, S. W. Hu, J. Wang, and T. Y. Wang. High-temperature behavior of polyvinyl alcohol fiber-reinforced metakaolin/ fly ash-based geopolymer mortar. Composites Part B-Engineering, Vol. 244, 2022, id. 110171.
- [22] Mo, L. W., L. M. Lv, M. Deng, and J. S. Qian. Influence of fly ash and metakaolin on the microstructure and compressive strength of magnesium potassium phosphate cement paste. Cement and Concrete Research, Vol. 111, 2018, pp. 116-129.
- [23] Zhang, P., K. X. Wang, J. Wang, J. J. Guo, and Y. F. Ling. Macroscopic and microscopic analyses on mechanical performance of metakaolin/fly ash based geopolymer mortar. Journal of Cleaner Production, Vol. 294, 2021, id. 126193.
- [24] Li, X. Y., C. Y. Bai, Y. J. Qiao, X. D. Wang, K. Yang, and P. Colombo. Preparation, properties and applications of fly ash-based porous geopolymers: A review. Journal of Cleaner Production, Vol. 359, 2022, id. 132043.
- [25] Zhang, P., S. Y. Wei, Y. X. Zheng, F. Wang, and S. W. Hu. Effect of single and synergistic reinforcement of PVA fiber and nano-SiO₂ on workability and compressive strength of geopolymer composites. Polymers, Vol. 14, 2022, id. 3765.
- [26] Jithendra, C., V. N. Dalawai, and S. Elavenil. Effects of metakaolin and sodium silicate solution on workability and compressive strength of sustainable geopolymer mortar. 2nd International Conference on Sustainable Energy Solutions for a Better Tomorrow (SESBT), Elsevier, Vellore Inst Technol, Chennai, India, 2021. p. 1580-1584.
- [27] Guo, X. L. and G. Y. Xiong. Resistance of fiber-reinforced fly ashsteel slag based geopolymer mortar to sulfate attack and dryingwetting cycles. Construction and Building Materials, Vol. 269, 2021, id. 121326.
- [28] Abdalla, A. and A. S. Mohammed. Surrogate models to predict the long-term compressive strength of cement-based mortar modified with fly ash. Archives of Computational Methods in Engineering, Vol. 29, 2022, pp. 4187-4212.
- [29] Gao, Z., P. Zhang, J. J. Guo, and K. X. Wang. Bonding behavior of concrete matrix and alkali-activated mortar incorporating nano-SiO₂ and polyvinyl alcohol fiber: theoretical analysis and prediction model. Ceramics International, Vol. 47, 2021, pp. 31638-31649.
- Abdalla, A. and A. S. Mohammed. Hybrid MARS-, MEP-, and ANNbased prediction for modeling the compressive strength of cement mortar with various sand size and clay mineral metakaolin content. Archives of Civil and Mechanical Engineering, Vol. 22, 2022, id. 194.
- [31] Zhang, P., S. Y. Wei, J. J. Wu, Y. Zhang, and Y. X. Zheng. Investigation of mechanical properties of PVA fiber-reinforced cementitious

- composites under the coupling effect of wet-thermal and chloride salt environment. *Case Studies in Construction Materials*, Vol. 17, 2022, id. e01325.
- [32] Guo, X. L., J. Y. Yang, and G. Y. Xiong. Influence of supplementary cementitious materials on rheological properties of 3D printed fly ash based geopolymer. *Cement & Concrete Composites*, Vol. 114, 2020. id. 103820.
- [33] Korniejenko, K., W. T. Lin, and H. Simonova. Mechanical properties of short polymer fiber-reinforced geopolymer composites. *Journal* of Composites Science, Vol. 4, 2020, id. 128.
- [34] Mohammed, A., A. Salih, and H. Raof. Vipulanandan constitutive models to predict the rheological properties and stress-strain behavior of cement grouts modified with metakaolin. *Journal of Testing and Evaluation*. Vol. 48, 2020. pp. 3925–3945.
- [35] Abdalla, A. and A. Salih. Microstructure and chemical characterizations with soft computing models to evaluate the influence of calcium oxide and silicon dioxide in the fly ash and cement kiln dust on the compressive strength of cement mortar. *Resources*, *Conservation & Recycling Advances*, Vol. 15, 2022, id. 200090.
- [36] Mobili, A., A. Belli, C. Giosue, T. Bellezze, and F. Tittarelli. Metakaolin and fly ash alkali-activated mortars compared with cementitious mortars at the same strength class. *Cement and Concrete Research*, Vol. 88, 2016, pp. 198–210.
- [37] Ishwarya, G., B. Singh, S. Deshwal, and S. K. Bhattacharyya. Effect of sodium carbonate/sodium silicate activator on the rheology, geopolymerization and strength of fly ash/slag geopolymer pastes. *Cement & Concrete Composites*, Vol. 97, 2019, pp. 226–238.
- [38] Gao, Z., P. Zhang, J. Wang, K. X. Wang, and T. H. Zhang. Interfacial properties of geopolymer mortar and concrete substrate: effect of polyvinyl alcohol fiber and nano-SiO₂ contents. *Construction and Building Materials*, Vol. 315, 2022, id. 125735.
- [39] Ahmad, M. R., B. Chen, M. A. Haque, and S. Y. Oderji. Multiproperty characterization of cleaner and energy-efficient vegetal concrete based on one-part geopolymer binder. *Journal of Cleaner Production*, Vol. 253, 2020, id. 119916.
- [40] Youssf, O., J. E. Mills, M. Elchalakani, F. Alanazi, and A. M. Yosri. Geopolymer concrete with lightweight fine aggregate: material performance and structural application. *Polymers*, Vol. 15, 2023, id. 171.
- [41] Korniejenko, K., P. Kejzlar, and P. Louda. The influence of the material structure on the mechanical properties of geopolymer composites reinforced with short fibers obtained with additive technologies. *International Journal of Molecular Sciences*, Vol. 23, 2022, id. 2023.
- [42] Sun, Z. Q. and A. Vollpracht. One year geopolymerisation of sodium silicate activated fly ash and metakaolin geopolymers. *Cement & Concrete Composites*, Vol. 95, 2019, pp. 98–110.
- [43] Duan, P., C. J. Yan, and W. Zhou. Influence of partial replacement of fly ash by metakaolin on mechanical properties and microstructure of fly ash geopolymer paste exposed to sulfate attack. *Ceramics International*, Vol. 42, 2016, pp. 3504–3517.
- [44] Zhang, Z. H., H. Wang, Y. C. Zhu, A. Reid, J. L. Provis, and F. Bullen. Using fly ash to partially substitute metakaolin in geopolymer synthesis. *Applied Clay Science*, Vol. 88-89, 2014, pp. 194–201.
- [45] Zhang, P., Y. X. Sun, F. Wang, and J. Wang. Mechanical properties and durability of geopolymer recycled aggregate concrete: A review. *Polymers*, Vol. 15, 2023, id. 615.
- [46] Bowen, F., L. Jiesheng, W. Jing, C. Yaohua, Z. Tongtong, T. Xiaoming, et al. Investigation on the impact of different activator to solid ratio

- on properties and micro-structure of metakaolin geopolymer. *Case Studies in Construction Materials*, Vol. 16, 2022, id. e01127.
- [47] Kanagaraj, B., N. Anand, R. S. Raj, and E. Lubloy. Performance evaluation of sodium silicate waste as a replacement for conventional sand in geopolymer concrete. *Journal of Cleaner Production*, Vol. 375, 2022, id. 134172.
- [48] Huang, W. and H. Wang. Multi-aspect engineering properties and sustainability impacts of geopolymer pervious concrete. *Composites Part B-Engineering*, Vol. 242, 2022, id. 110035.
- [49] Youssf, O., M. Elchalakani, R. Hassanli, R. Roychand, Y. Zhuge, R. J. Gravina, et al. Mechanical performance and durability of geopolymer lightweight rubber concrete. *Journal of Building Engineering*, Vol. 45, 2022, id. 103608.
- [50] JGJ/T70-2009. Standard for test method of performance on building mortar [in Chinese], China Architecture and Building Press, Beijing, China, 2009.
- [51] GB/T7897-2008. Test methods of mechanical properties of mortar for ferrocement [in Chinese], China Standard Press, Beijing, China, 2008.
- [52] GB/T-50082-2009. Standard for test methods of long-term performance and durability of ordinary concrete [in Chinese], China Architecture and Building Press, Beijing, China, 2009.
- [53] JC/T951-2005. Test method for cracking-resistance of cement mortar [in Chinese], China Architecture and Building Press, Beijing, China, 2005.
- [54] Mermerdas, K., Z. Algin, and S. Ekmen. Experimental assessment and optimization of mix parameters of fly ash-based lightweight geopolymer mortar with respect to shrinkage and strength. *Journal of Building Engineering*, Vol. 31, 2020, id. 101351.
- [55] Shah, S. F. A., B. Chen, M. R. Ahmad, and M. A. Haque. Development of cleaner one-part geopolymer from lithium slag. *Journal of Cleaner Production*, Vol. 291, 2021, id. 125241.
- [56] Luo, Y., Z. Jiang, D. Wang, Y. Lv, C. Gao, and G. Xue. Effects of alkaline activators on pore structure and mechanical properties of ultrafine metakaolin geopolymers cured at room temperature. *Construction and Building Materials*, Vol. 361, 2022, id. 129678.
- [57] Ghafoor, M. T., Q. S. Khan, A. U. Qazi, M. N. Sheikh, and M. N. S. Hadi. Influence of alkaline activators on the mechanical properties of fly ash based geopolymer concrete cured at ambient temperature. *Construction and Building Materials*, Vol. 273, 2021, id. 121752.
- [58] Duxson, P., S. W. Mallicoat, G. C. Lukey, W. M. Kriven, and J. S. J. van Deventer. The effect of alkali and Si/Al ratio on the development of mechanical properties of metakaolin-based geopolymers. *Colloids and Surfaces a-Physicochemical and Engineering Aspects*, Vol. 292, 2007, pp. 8–20.
- [59] Ryu, G. S., Y. B. Lee, K. T. Koh, and Y. S. Chung. The mechanical properties of fly ash-based geopolymer concrete with alkaline activators. *Construction and Building Materials*, Vol. 47, 2013, pp. 409–418.
- [60] Chen, X. D., S. X. Wu, and J. K. Zhou. Influence of porosity on compressive and tensile strength of cement mortar. *Construction and Building Materials*, Vol. 40, 2013, pp. 869–874.
- [61] Choi, Y. and R. L. Yuan. Experimental relationship between splitting tensile strength and compressive strength of GFRC and PFRC. Cement and Concrete Research, Vol. 35, 2005, pp. 1587–1591.
- [62] Shariati, M., A. Shariati, N. T. Trung, P. Shoaei, F. Ameri, N. Bahrami, et al. Alkali-activated slag (AAS) paste: Correlation between durability and microstructural characteristics. *Construction and Building Materials*, Vol. 267, 2021, id. 120886.
- [63] Atabey, O. II, C. Karahan, C. Bilim, and C. D. Atis. The influence of activator type and quantity on the transport properties of class F fly

- ash geopolymer. *Construction and Building Materials*, Vol. 264, 2020, id. 120268.
- [64] Hedegaard, S. E. and T. C. Hansen. Water permeability of fly-ash concretes. *Materials and Structures*, Vol. 25, 1992, pp. 381–387.
- [65] Wang, L., R. Y. Luo, W. Zhang, M. M. Jin, and S. W. Tang. Effects of fineness and content of phosphorus slag on cement hydration, permeability, pores structure and fractal dimension of concrete. Fractals-Complex Geometry Patterns and Scaling in Nature and Society, Vol. 29, 2021, id. 2140004.
- [66] Yu, Z. Q., C. X. Ni, M. L. Tang, and X. D. Shen. Relationship between water permeability and pore structure of Portland cement paste blended with fly ash. *Construction and Building Materials*, Vol. 175, 2018, pp. 458–466.
- [67] Wang, L., R. Y. Luo, W. Zhang, M. M. Jin, and S. W. Tang. Effects of fineness and content of phosphorus slag on cement hydration, permeability, pore structure and fractal dimension of concrete. Fractals-Complex Geometry Patterns and Scaling in Nature and Society, Vol. 29, 2021, id. 2140004.
- [68] Wang, L., X. M. Zeng, Y. Li, H. M. Yang, and S. W. Tang. Influences of MgO and PVA fiber on the abrasion and cracking resistance, pore structure and fractal features of hydraulic concrete. *Fractal and Fractional*, Vol. 6, 2022, id. 674.
- [69] Sant, G., D. Bentz, and J. Weiss. Capillary porosity depercolation in cement-based materials: measurement techniques and factors which influence their interpretation. *Cement and Concrete Research*, Vol. 41, 2011, pp. 854–864.
- [70] Garboczi, E. J. Permeability, diffusivity, and microstructural parameters: A critical review. *Cement and Concrete Research*, Vol. 20, 1990, pp. 591–601.
- [71] Wang, L., X. Lu, L. S. Liu, J. Xiao, G. Zhang, F. X. Guo, et al. Influence of MgO on the hydration and shrinkage behavior of low heat Portland cement-based materials via pore structural and fractal analysis. *Fractal and Fractional*, Vol. 6, 2022, id. 40.

- [72] Huang, J. S., W. W. Li, D. S. Huang, L. Wang, E. Chen, C. Y. Wu, et al. Fractal analysis on pore structure and hydration of magnesium oxysulfate cements by first principle, thermodynamic and microstructure-based methods. *Fractal and Fractional*, Vol. 5, 2021, id. 164.
- [73] Abdalla, A. A. and A. S. Mohammed. Theoretical models to evaluate the effect of SiO₂ and CaO contents on the long-term compressive strength of cement mortar modified with cement kiln dust (CKD). Archives of Civil and Mechanical Engineering, Vol. 22, 2022, id. 105.
- [74] Qadir, W., K. Ghafor, and A. Mohammed. Characterizing and modeling the mechanical properties of the cement mortar modified with fly ash for various water-to-cement ratios and curing times. Advances in Civil Engineering, Vol. 2019, 2019, id. 7013908
- [75] Karaaslan, C., E. Yener, T. Bagatur, R. Polat, R. Gul, and M. H. Alma. Synergic effect of fly ash and calcium aluminate cement on the properties of pumice-based geopolymer mortar. *Construction and Building Materials*, Vol. 345, 2022, id. 128397.
- [76] Hou, L., J. Li, and Z. Y. Lu. Effect of Na/Al on formation, structures and properties of metakaolin based Na-geopolymer. *Construction and Building Materials*, Vol. 226, 2019, pp. 250–258.
- [77] Kelestemur, O., S. Yildiz, B. Gokcer, and E. Arici. Statistical analysis for freeze-thaw resistance of cement mortars containing marble dust and glass fiber. *Materials & Design*, Vol. 60, 2014, pp. 548–555.
- [78] Yan, D. M., S. K. Chen, Q. Zeng, S. L. Xu, and H. D. Li. Correlating the elastic properties of metakaolin-based geopolymer with its composition. *Materials & Design*, Vol. 95, 2016, pp. 306–318.
- [79] Biswal, U. S. and P. Dinakar. Influence of metakaolin and silica Fume on the mechanical and durability performance of highstrength concrete made with 100% coarse recycled aggregate. *Journal of Hazardous, Toxic, and Radioactive Waste*, Vol. 26, 2022, id. 04022004.